A high pressure x-ray diffraction study of titanium disulfide

2009 J. Phys.: Condens. Matter 21 025403

(http://iopscience.iop.org/0953-8984/21/2/025403)

J. Phys.: Condens. Matter **21** (2009) 025403 (5pp) doi:10.1088/0953-8984/21/2/025403

A high pressure x-ray diffraction study of titanium disulfide

Resul Aksoy, Emre Selvi, Russell Knudson and Yanzhang Ma

Department of Mechanical Engineering, Texas Tech University, Lubbock, TX 79409, USA

E-mail: y.ma@ttu.edu

Received 15 May 2008, in final form 8 October 2008
Published 10 December 2008
Online at stacks.iop.org/JPhysCM/21/025403

Abstract

A high pressure angle dispersive synchrotron x-ray diffraction study of titanium disulfide (TiS_2) was carried out to pressures of 45.5 GPa in a diamond-anvil cell. We observed a phase transformation of TiS_2 beginning at about 20.7 GPa. The structure of the high pressure phase needs further identification. By fitting the pressure–volume data to the third-order Birch–Murnaghan equation of state, the bulk modulus, K_{0T}, was determined to be 45.9 ± 0.7 GPa with its pressure derivative, K'_{0T}, being 9.5 ± 0.3 at pressures lower than 17.8 GPa. It was found that the compression behavior of TiS_2 is anisotropic along the different axes. The compression ratio of the c-axis is about nine times larger than the a-axis when pressures are lower than 1 GPa. It suddenly decreases to three times larger at pressures of about 3 GPa. This ratio shows a linear decrease with a slope of negative 0.048 at pressures below phase transformation.

1. Introduction

TiS_2, one of the most studied structures among the transition-metal dichalcogenides (TMDCs), attracts considerable attention due to its structural properties and potential use in a variety of technological applications. TMDCs consist of two hexagonally close-packed layers between which the transition metals exist in either prismatic (2H) or octahedral (1T) coordination of six chalcogens (sulfur or selenium). TiS_2 with the most stable form, 1T polytype, has a highly anisotropic structure with a space group $P\bar{3}m1$ formed from infinite layers of face-sharing TiS_6 octahedra [1], as shown in figure 1. Inside the single layers each Ti ion is surrounded octahedrally, coordinated by six S ions forming S–Ti–S sandwich layers, where a sheet of Ti atoms is sandwiched between two sulfur sheets. Atoms within the S–Ti–S layers are bound by strong covalent bonds, while individual S–Ti–S layers are held together by van der Waals interactions only.

In applications, the introduction of different atoms or molecules, various electron donors such as alkali metals and organic molecules, between the layers is enabled by intercalation [2, 3]. A positive electrode of lithium can be intercalated between the S–Ti–S inter-layers [4], and this new compound is used as a rechargeable lithium battery [4–6]. TiS_2 can also be utilized as a hydrogen storage material. Chen *et al* [7] reported that TiS_2 nanotubes can efficiently store 2.5 wt% of hydrogen at a temperature of 298 K and under a hydrogen pressure of 4 MPa. In early publications about TiS_2, there was controversy over whether it is a semimetal or a semiconductor. Logothetis *et al* [8] have reported that TiS_2 is a semiconductor at ambient pressure. Allan *et al* concluded that TiS_2 changes from a semiconductor to a semimetal in compression to 8 GPa [9]. In the study of Allan and Sangeeta Sharma *et al* [10], they calculated the cell parameters of TiS_2 under high pressure to about 8 GPa, and no phase transformation was observed in the pressure range.

Our study presents high pressure x-ray measurements on TiS_2 up to 45.5 GPa which reveals that the phase transformation begins at about 20.7 GPa.

2. Experimental details

The *in situ* high pressure synchrotron x-ray diffraction experiments were carried out on TiS_2 powder using a symmetrical diamond-anvil cell at room temperature. The culet diameters of the diamonds were 300 μm. The sample was ground into fine grains and compressed to form a flake before it was loaded. In order to avoid bridging between diamond culets at high pressures a smaller portion of the sample, about one-third the size of the sample chamber, was inserted. A T-301 stainless steel gasket was indented to 20 GPa. A hole of 120 μm diameter was drilled in the center of the indentation by an electric discharge machine. The hole was large enough

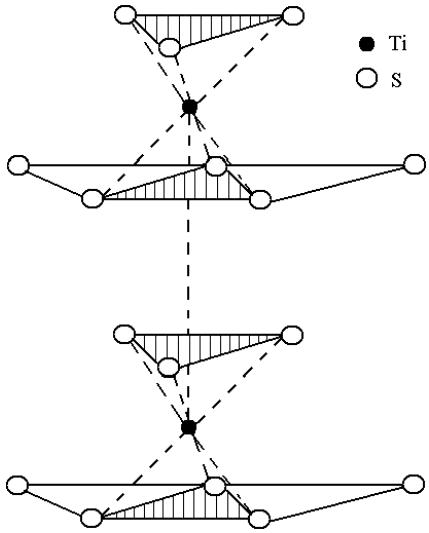

Figure 1. The crystal structure of hexagonal TiS_2, showing the arrangement of sulfur atoms (open circles) and titanium atoms (solid circles).

with respect to the size of the x-ray beam to avoid diffraction from the gasket. A mixture of methanol–ethanol at a 4:1 volume ratio (M–E) was used as a pressure medium. A few ruby chips were loaded at different positions of the sample for pressure calibration. The ruby luminescence technique was used to determine the pressure from the shift of the ruby R_1 fluorescence line [11]. The TiS_2 sample was from Alfa Aesar Co. with 99.8% purity.

The high pressure angle dispersive x-ray diffraction (ADXRD) measurements were performed at Beam Line X17C, Brookhaven National Laboratory. The angle dispersive imaging plate method was used with an x-ray wavelength of 0.4066 Å. The x-ray beam was focused to a dimension of $20 \times 25\ \mu m^2$. The exposure time for the diffraction patterns was approximately 25 min. After exposure, the image was read using a Fuji Image Reader (BAS-2500) with $100\ \mu m \times 100\ \mu m$ resolution.

3. Results and discussion

Two-dimensional ring patterns were processed using the program FIT2D [12] in order to produce the intensity versus 2θ plot. A software program, Peakfit v4.11, was used to analyze the diffraction patterns and determine peak positions at different pressures. The conversion from angle to d-spacings was based on the formula $d = \frac{\lambda}{2\times\sin(\theta)}$, where λ is the x-ray wavelength in Å, d is the d-spacing in Å, and θ is the diffraction angle in degrees [13]. From the ADXRD measurements, the x-ray diffraction patterns shown in figure 2 were collected up to 45.5 GPa. The first pattern was taken under 0 GPa without using the diamond-anvil cell. This is the reason why the intensity of the peaks is high when compared with the peaks under pressure. These patterns are representative of selected pressures. The diffraction patterns show some distortion with increasing pressures. This might be caused by surface disorder at higher pressures. A new peak

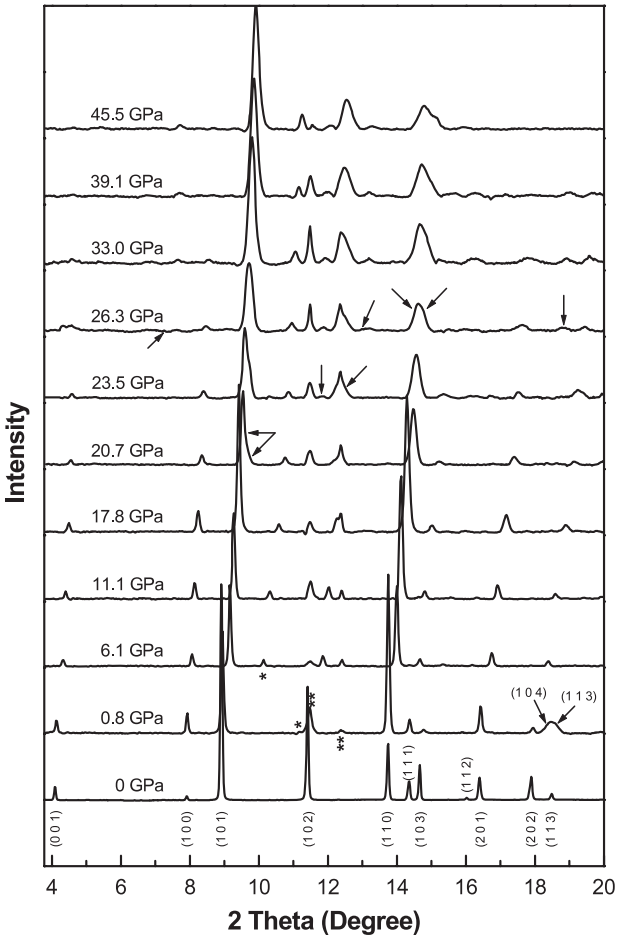

Figure 2. Angle dispersive x-ray diffraction patterns of TiS_2 at selected pressures. The numbers in parenthesis under the first pattern are the corresponding Miller indices of TiS_2. The asterisk on the second and third patterns marks the diffraction from ruby. A double asterisk indicates systematic error. New peaks are shown with arrows above 17.8 GPa.

arises between the (0 0 1) and (1 0 0) peaks at 26.3 GPa. The (0 0 1) and (1 0 0) peaks disappear at 39.0 GPa. The peaks (1 0 1) and (1 1 0) start broadening at 17.8 GPa, then split into two at 20.7 GPa and 26.3 GPa, respectively. The (1 0 2) peak shifts to the left at 20.7 GPa, then splits into two at 23.5 GPa. Another new peak shows up between the (1 0 2) and (1 1 0) peaks at 26.3 GPa. The (2 0 1) peak becomes broader at 17.8 GPa, but we cannot say that it splits into two peaks. Between the (2 0 1) and (2 0 2) peaks, a new peak arises at 26.3 GPa. A new peak is an indication of a change in the structure. The splitting of some peaks indicates that a phase transformation has occurred. But the structure of high pressure phase has not been identified yet.

Diffraction images from TiS_2 at selected pressures are shown in figure 3. The image at 23.5 GPa shows that the (101) peak broadened widely. And two peaks are required to give a good fit when Peakfit software is used to find a proper fit at this pressure. As mentioned previously, it can also be seen that the (1 1 0) peak broadens at 17.8 GPa. The pressure dependency of the d-spacings is illustrated in figure 4. All of the d-spacings decrease linearly at an almost similar rate with

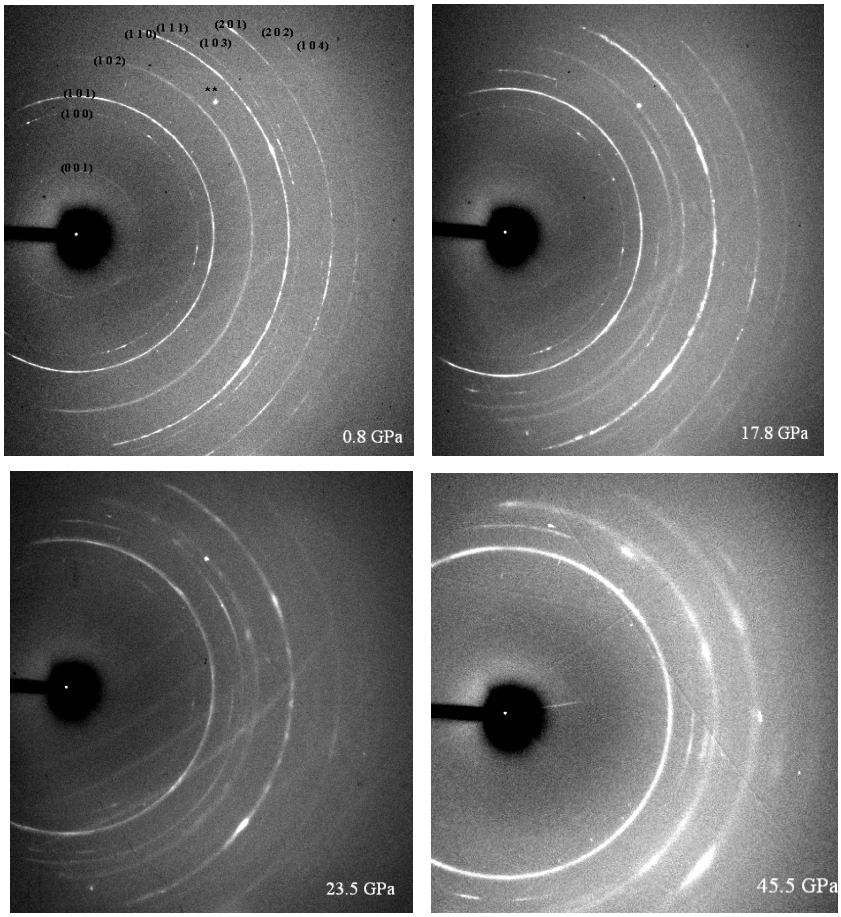

Figure 3. X-ray diffraction images of the TiS_2 sample. The numbers in parenthesis on the images are the corresponding Miller indices of TiS_2.

increasing pressure, but the (0 0 1) plane vibrating in the c-axis shows a different curvature with higher rate of reduction of d-spacing. This figure was divided into two different parts, indicating before and after phase transformation. At pressures above 17.8 GPa, a phase transformation is evident by the appearance of additional peaks. The pressure dependency of cell parameters of TiS_2, compared with molybdenum disulfide (MoS_2) and tungsten disulfide (WS_2) data, is shown in figure 5. The lattice parameters were determined up to 17.8 GPa for TiS_2. It is noted that the compression behavior of TiS_2 is anisotropic. The a-axis decreases by 4% and the c-axis decreases by 9.5% at 17.8 GPa. Due to weak van der Waals bonds keeping S and Ti atoms together, the c-axis is more compressible than the a-axis. The ratio of axial reduction between the a-axis and the c-axis for TiS_2, MoS_2, and WS_2 is illustrated in figure 6. The c-axis compression ratio of TiS_2 is about nine times larger than the a-axis one at pressures below 1 GPa, then decreases to three times larger at pressures below 4 GPa. This ratio shows a nearly linear decrease with a slope of negative 0.048 at pressures below phase transformation. The difference in compression of a/a_0 and c/c_0 and the ratio of axial reduction between TiS_2 and MoS_2 might be caused by cations. But the WS_2 data show less reduction which might be caused by nonhydrostatic compression (no pressure medium) [14]. The V/V_0 (V is volume at P pressure, and V_0 is the volume at ambient pressure) relation of TiS_2 as a function of pressure is shown and compared in figure 7. The relative volume change of TiS_2 was compared with MoS_2 and WS_2. By fitting the pressure–volume data to the third-order Birch–Murnaghan equation of state, the bulk modulus for TiS_2 was determined to be 45.9 ± 0.7 GPa, with its pressure derivative K'_{0T} being 9.5 ± 0.3 below 17.78 GPa. The 'bulk' software, written by Downs, was used to determine the bulk modulus values. It is found that TiS_2 is softer and more compressible than MoS_2 and WS_2. The difference in cation atoms (Ti, Mo, and W) could be the main effect on the compressibility. The experiment with WS_2 with no pressure medium, causing nonhydrostatic compression, might have produced an inaccurate measurement in determining bulk modulus.

4. Conclusion

TiS_2 has been studied by synchrotron angle dispersive x-ray diffraction to 45.5 GPa. The pressure–volume data were fitted to the third-order Birch–Murnaghan equation of state and the bulk modulus was found to be $K_{0T} = 45.9 \pm 0.7$ GPa, with its pressure derivative $K'_{0T} = 9.5 \pm 0.3$ below 17.78 GPa. It is noted that TiS_2 shows anisotropic compression behavior. We have observed that the phase transformation of TiS_2 begins at about 20.7 GPa. The structure of the high pressure phase

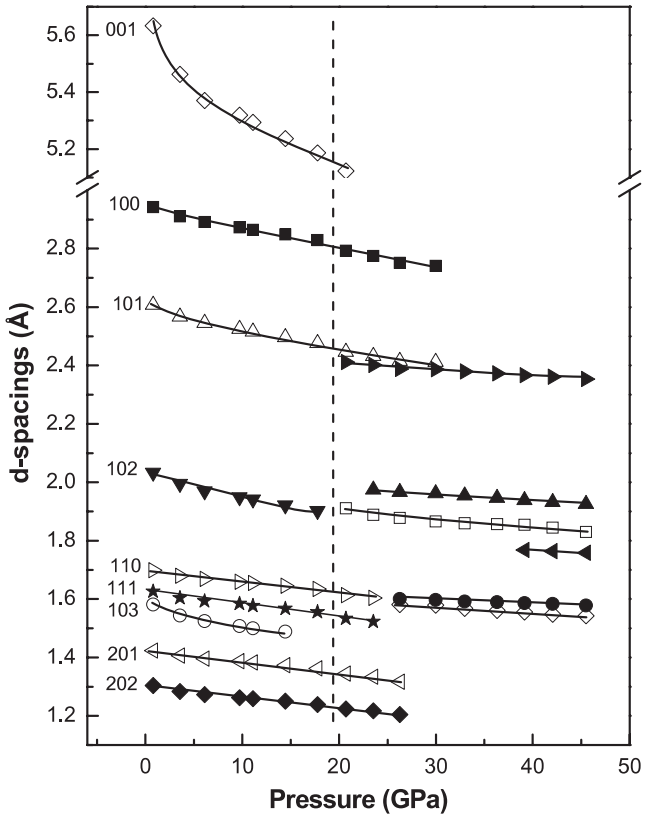

Figure 4. The change in d-spacings as a function of pressure. The solid lines on the data show the fitting to first or second order of pressure. The straight dashed line shows the division before and after the phase transformation.

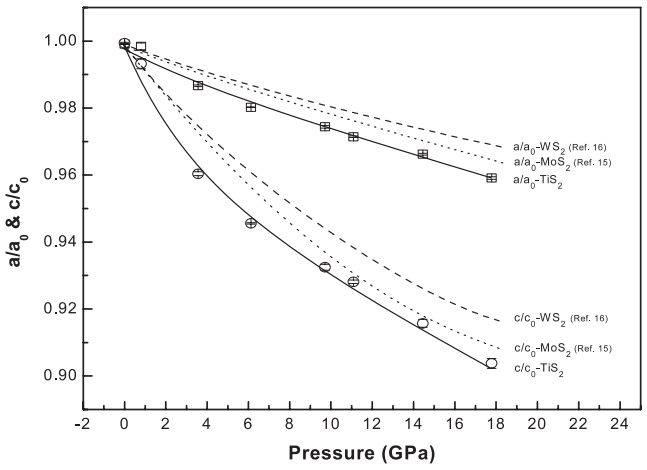

Figure 5. Pressure dependence of the unit cell parameter. The solid lines are a guide to the eyes. The refinement errors are within the symbols. The unit cell, of dimensions $a = 3.407$ Å, $c = 5.695$ Å, are given by ICDD-JCPDS card no. 15-0853. The dotted and dashed lines represent MoS_2 [15] and WS_2 [16], respectively.

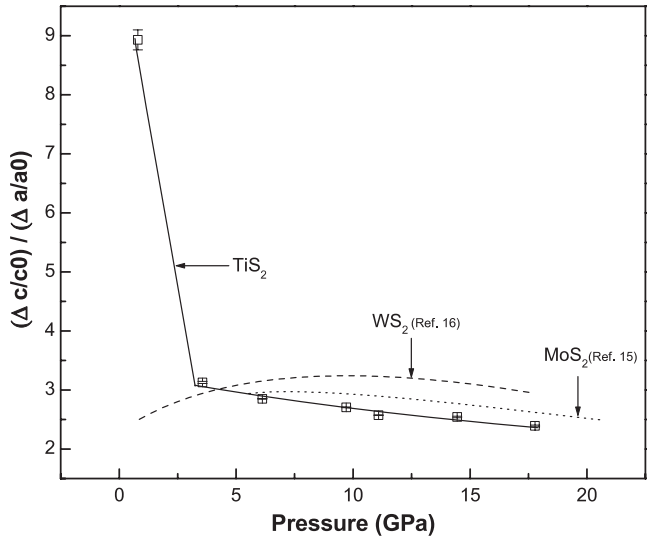

Figure 6. The ratio of axial reduction between the c- and a-axis at pressures. Solid square symbols represent the data for TiS_2. The dotted and dashed lines represent MoS_2 [15] and WS_2 [16], respectively.

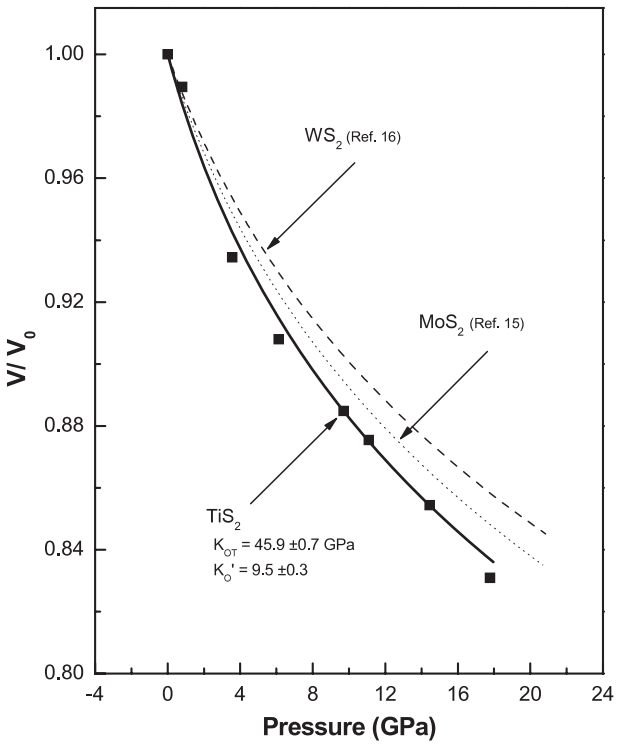

Figure 7. Pressure dependence of the relative unit cell volume of TiS_2. The curve fitted to the third-order Birch–Murnaghan (B–M) equation of state (EOS) is shown with a solid line. The dotted and dashed lines represent MoS_2 [15] and WS_2 [16] curves fitted to the third-order B–M EOS, respectively.

needs further identification. The c-axis compression ratio is four and three times larger than the a-axis at pressures below 1 and 4 GPa, respectively. Then it almost linearly decreases with slope of negative 0.048 at pressures below phase transformation. It is noted that TiS_2 is softer and more compressible than MoS_2 and WS_2.

Acknowledgments

We are grateful to J Hu and Q Guo for their technical support with the x-ray diffraction measurements at Brookhaven National Laboratory.

References

[1] Riekel C and Schollhorn R 1975 *Mater. Res. Bull.* **10** 629
[2] Friend R H and Yoffe A D 1987 *Adv. Phys.* **36** 1
[3] Liang W Y 1986 *Intercalation in Layered Materials* (*NATO Advanced Study Institute Series B: Physics* vol 148) ed M S Dresselhaus (New York: Plenum)
[4] Whittingham M S 1976 *Science* **192** 1126
[5] Scrosati B 1995 *Nature* **373** 557
[6] Armstrong A R and Bruce P G 1996 *Nature* **381** 499
[7] Chen J, Li S L, Tao Z L, Shen Y T and Cui C X 2003 *J. Am. Chem. Soc.* **125** 5284–5
[8] Wu Z Y, Lemoigno F, Gressier P, Ouvrard G, Moreau P, Rouxel J and Natoli C R 1996 *Phys. Rev.* B **54** 11009
[9] Allan D R *et al* 1998 *Phys. Rev.* B **57** 5106
[10] Sangeeta S, Nautiyal T, Singh G S, Auluck S, Blaha P and Ambrosch-Draxl C 1999 *Phys. Rev.* B **59** 14833
[11] Mao H K, Xu J and Bell P M J 1986 *Geophys. Res.* **91** 4673–6
[12] Hammersley A P, Svensson S O, Hanfland M, Fitch A N and Häusermann D 1996 *High Pressure Res.* **14** 235
[13] Suryanarayana C and Grant Norton M 1998 *X-Ray Diffraction: a Practical Approach* (New York: Plenum)
[14] Liu H, Hu J, Shu J, Häusermann D and Mao H K 2004 *Appl. Phys. Lett.* **85** 1973
[15] Aksoy R, Ma Y, Selvi E, Chyu M C, Ertas A and White A 2006 *J. Phys. Chem. Solids* **67** 1914
[16] Selvi E, Ma Y, Aksoy R, Ertas A and White A 2006 *J. Phys. Chem. Solids* **67** 2183